Shape-Selective Assembly in Deformable Systems using Templated Assembly by Selective Removal

G. Agarwal[1], A. Servi, F. Eid, C. Livermore[2]
Massachusetts Institute of Technology, Department of Mechanical Engineering

Abstract

This paper presents the first experimental demonstration of deformable polymer microspheres assembling selectively on rigid assembly templates using Templated Assembly by Selective Removal (TASR). Polystyrene microspheres with 2 μm diameter were successfully assembled on patterned, oxidized silicon templates having uniformly well-matched assembly sites with 100% assembly yield. Experiments also demonstrated selective filling of different assembly site sizes/shapes interleaved into a single array. In order to address the effects of deformability theoretically, a model was created to assess the applicability of TASR to different materials systems using Hertzian contact theory to identify the onset of plastic deformation in a loaded, deformable sphere. Based on this model, TASR's effectiveness was predicted to include some polymers on rigid substrates. Quantitative comparison of the data on assembly of deformable systems with existing TASR models for non-deformable systems shows significant though not complete agreement.

[1] Gunjan Agarwal, 77 Massachusetts Avenue, Room 3-455 C, Cambridge, MA-02139, USA
Ph. 617-253-5589, E-mail: agarwalg@mit.edu

[2] Prof. Carol Livermore, 77 Massachusetts Avenue, Room 3-449 C, Cambridge, MA-02139, USA
Ph. 617-253-6761, E-mail: livermor@mit.edu

1. Introduction

Templated Assembly by Selective Removal (TASR) is a unique approach to self assembly that relies on a fundamentally shape and size selective mechanism for assembling components at the micro and nano scales. TASR enables simultaneous assembly of diverse components into complex and highly precise systems with a range of potential applications. TASR may be used either as a permanent or as a reversible assembly process, enabling its use not only for construction of final systems but also for applications such as chromatography.

TASR employs a combination of chemistry, surface topography and controllable ultrasonically-induced fluid forces to assemble diverse sets of objects selectively from fluid into designated sites on a 2D surface [1 -3]. Figure 1 is a schematic diagram of the assembly set-up. The components and substrate, after undergoing chemical surface modification by coating with an adhesion promoter, are placed in a fluid environment for the assembly process, and megahertz frequency ultrasound is applied to the fluid. Competition between the chemical adhesive effects and fluidic removal effects drive the selective assembly. Components remain assembled in a given assembly site when adhesive effects are stronger than removal effects; otherwise, they are removed. The assembly selectivity (that is, whether adhesive or removal effects are dominant) depends on the degree to which the component to be assembled matches the shape and dimensions of the surface topography at that location. The surface topography is designed such that holes at various locations in the substrate surface match the shapes of the components that are intended to assemble there.

The TASR concept has been demonstrated previously with silica microspheres assembled on patterned silicon substrates, and a model has been created to explain the assembly of rigid components on a rigid substrate [1-3]. Because TASR depends on shape and size matching between surfaces, the assembly of more deformable materials (i.e. materials in which deformation can change the degree of apparent shape matching between component and substrate) is more challenging. The current work presents analysis and experiments on the extension of the TASR technique to deformable materials. Such materials may be used for applications ranging from assembling functionalized polymer particles for chemical or biological sensors, to creation of optical metamaterials, to shape- and size-based sorting of biological

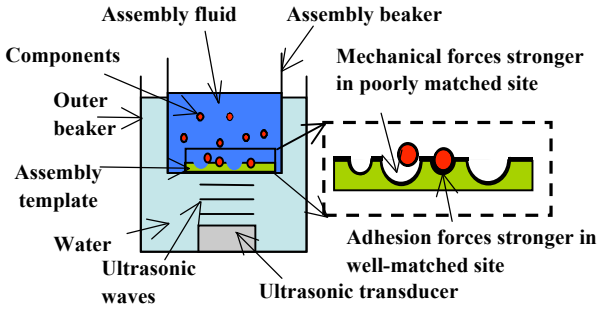

Fig. 1: Schematic illustration of the experimental set-up for TASR including the assembly bath (in which variable chemistry and shape matching are implemented through the choice of materials and component/template geometry) and the 1.7 MHz ultrasonic transducer that introduces mechanical forces to the selective removal system

materials such as cells. For simplicity, assembly of deformable materials will be considered here for spherical components; however the analysis and techniques are readily extendable to many non-spherical shapes.

2. Predictive Model for TASR

The original TASR model explains the selective assembly process as a combination of random assembly and selective removal [1-3]. According to the model, which fits the data well for rigid components and assembly substrates, whether a component will be assembled in a given site is effectively predicted by whether the mechanical moments (caused by the acoustic fluid excitation) that tend to roll a given component out of a given assembly site hole on the substrate surface are greater than the mechanical moments (caused by chemical adhesion) that tend to oppose removal of the component from the hole. The introduction of either deformable substrate templates or deformable components introduces a new set of considerations, since deformation can change the degree of shape matching between component and substrate, and hence may change how assembly yield depends on how well the undeformed component matches the undeformed assembly site.

Here we introduce a modified TASR theory that takes into account the mechanical properties of the components and substrate. The theory rests on a simple energy argument. Self assembly in general and TASR in particular depend on the tendency of systems to minimize their free energy. If the deformation of components and substrate are fully elastic, any reduction in system free energy due to the increase in contact area upon deformation will equal the increase in system free energy due to the storage of elastic energy in the deformed structures. Therefore, for purely elastic deformations, the original TASR model should still apply. In contrast, if the deformation enters the plastic regime, some of the energy will be dissipated, and the TASR model should no longer apply completely. Therefore, the ability to assemble deformable systems (with deformable components and/or substrate templates) comes down to the question of at what point the deformations enter the plastic regime. This in turn depends on a) the mechanical properties of the component and substrate materials, b) the magnitude of the force that holds the component on the substrate, and c) whether the component, the substrate, or both are deformable.

Although the same concept (the significance of the onset of plastic deformation) applies independent of whether it is the substrate, the components, or both that are deformable, the details of when plastic deformation sets in depend on which elements are deformable. This reflects the fact that there is a difference in constraint conditions between a small, deformable sphere (with a free opposite side) and a thicker, deformable plate (without a nearby space to readily accommodate the local deformation). Here we will consider only the case of deformable spherical components assembling on an essentially rigid substrate.

In the analysis that follows, the deformable material under consideration is assumed to be elastic-perfectly plastic with identical behavior in tension and compression. This is a good assumption for most of the materials that we have considered, such as silicon, glass or silica, aluminum, polystyrene, Polytetrafluoroethylene (PTFE), Poly methyl methacrylate (PMMA), and melamine. For a few materials, such as polydimethylsiloxane (PDMS) or biological cells,

additional forms of deformability such as viscoelasticity and hyperelasticity would need to be considered.

Hertzian elastic contact theory [4] is used to assess whether the component deformation is purely elastic or includes a plastic component. The theory that is employed here is strictly applicable either to two deformable spheres in contact, a deformable sphere in contact with a rigid flat, or to a deformable sphere in contact with a rigid sphere. It may also be approximately applied to the present situation of a deformable sphere inside a hole with a local (but not quite constant) radius of curvature. For assessing the applicability of the TASR process to a given materials system, the parameter of interest is the value of the critical interference ω_c that marks the transition from the purely elastic to the elastic-plastic deformation regime. Interference is a measure of the sphere's deformation and is equal to the difference between the sphere's radius and the distance from the center of the deformed sphere to the surface that it contacts. In other words, it is the amount by which the sphere would have had to penetrate into the second surface in order to approach it that closely in the absence of deformation. For values of the interference below the critical interference, the deformation is purely elastic and the original TASR theory is predicted to apply. For values of the interference above this value, the TASR theory is no longer entirely applicable.

The Hertzian closed-form expressions for the mechanics of two deformable spheres in purely elastic contact [4-7] can be used to determine the interference for a single elastic sphere in contact with a flat substrate (or indeed for a sphere in contact with a substrate with a given radius of curvature). The interference ω is given by

$$\omega = \left(\frac{\pi \cdot p_{\max}}{2E'} \right)^2 R_{eq} \tag{1}$$

where the equivalent radius R_{eq} is given in terms of the component radius R_c and the template's local radius of curvature R_t by

$$\frac{1}{R_{eq}} = \frac{1}{R_c} + \frac{1}{R_t}, \tag{2}$$

and the combined modulus E' is given in terms of the respective Young's moduli E_c and E_t and Poisson's ratios ν_c and ν_t of the components and template by

$$\frac{1}{E'} = \frac{\left(1-\upsilon_c^2\right)}{E_c} + \frac{\left(1-\upsilon_t^2\right)}{E_t}. \tag{3}$$

The term $p_{\max}$ is the maximum value of the contact pressure at the component/template contact.

The contact pressure arises from the net force that presses the component into the substrate template. This force is both chemical and fluidic in origin and is determined from the original TASR models [1-3]. If the contact between component and substrate template is approximated as a contact between two spherical surfaces, then the pressure may be taken to vary spatially as $\sqrt{1-r^2/a^2}$, where r is the radial distance out from the central contact point and a is the overall radius of the contact

area. Within this approximation, the maximum value of the contact pressure $p_{\max}$ is simply related to the average contact pressure p_{avg} as

$$p_{\max} = \frac{3}{2} p_{avg} = \frac{3}{2} \frac{F}{A}, \tag{4}$$

where the average pressure is the ratio of net force to contact area. According to Hertzian theory [4], the contact area between two elastic solids with spherical contact surfaces is given by

$$A = \pi a^2 = \pi \left(\frac{3 R_{eq} F}{4 E'} \right)^{2/3}. \tag{5}$$

Combining these results yields the value of the interference for the physical situation; this value is valid until the onset of plastic deformation but becomes invalid beyond it. The intererence ω is then compared with the critical interference value ω_c that marks the onset of plastic deformation. The critical interference has been calculated previously [8] to be

$$\omega_c = \left(\frac{\pi K H}{2 E'} \right)^2 R_{eq}, \tag{6}$$

where H is the hardness of the component and is related to its yield strength Y as

$$H = 2.8Y. \tag{7}$$

In Eq. 6, K refers to the hardness coefficient of the spherical component. The value of K was found in [9] by modeling based on finite element results. Their resulting values depend on Poisson's ratio and are given by

$$K = 0.454 + 0.41\nu_c. \tag{8}$$

Using these results, we are then able to calculate the ratio ω/ω_c of the interference to the critical interference for various component and substrate materials, and for various geometries (radii of curvature of spherical components and the template holes in which they assemble). If ω/ω_c is less than one, the original TASR model is predicted to be applicable, and the assembly is expected to be successful. If the calculated ratio exceeds one, then the TASR model will have begun to become invalid (though the discrepancy between the model and reality may be small for very small amounts of plastic deformation). In addition, for ratios above 1, it is known that the interference exceeds the critical interference, but not by how much, because this interference calculation is only strictly valid in the purely elastic regime. It is also important to note that the model described here takes into account only overall deformation of the sphere and not local deformations due to surface roughness.

The ω/ω_c ratios for some typical material combinations for the case of a 2 micron diameter sphere deforming on a flat surface are given in Table 1. For the examples described in the table, the template material is taken to be silicon dioxide for consistency with the experiments presented here. The ratios are well below the critical ratio of one both for Polytetrafluoroethylene (PTFE) and for Poly-methylmethacrylate

(PMMA) components on the relatively hard template substrate. However, the ratio is somewhat higher than one for polystyrene components on a relatively hard substrate, indicating that whether TASR can operate successfully and be well-described by the original model will depend strongly on the details of a given situation. The results will be somewhat different for different geometries, such as for a sphere that is not resting on a flat surface; the theoretical results for different geometries with polystyrene are discussed in comparison with the experimental results below.

Table 1. Ratios of interference to critical interference for different material combinations

Component material	**Template material**	ω/ω_c
PTFE (Teflon)	Silicon dioxide	0.090
PMMA	Silicon dioxide	0.079
Polystyrene	Silicon dioxide	1.3

3. Experimental Approach

The experimental protocols include the creation and functionalization of the templates on which assembly is to be carried out, the functionalization of the components that are to be assembled (when necessary), and the actual assembly experiments themselves. The relevant procedures are described below.

A) Template Fabrication

The templates for all of the experiments presented here comprise silicon dies coated with a layer of silicon dioxide into which the template holes (that is, the assembly sites) are etched. Fabrication of the patterned silicon template follows an approach that is nearly identical to the ones described in [1-3]. An oxidized silicon wafer is coated with polymethylmethacrylate (PMMA). In order to pattern hemispherical holes in the template, e-beam lithography is first used to expose various arrays of small spots in the PMMA resist layer with spot sizes ranging from 45 nm to 500 nm. Pattern development produces corresponding openings in the resist layer. The underlying oxide is then etched with buffered oxide etch (BOE) to produce isotropic holes. To lowest order, the isotropic etch produces hemispherical holes with hole radius approximately equal to the etch depth. The finite initial spot size results in etched holes that deviate slightly from the ideal hemispherical shape; the larger the initial spot size, the larger the deviation. Therefore, the holes with a smaller initial spot size will be a better fit for the spherical components, while the holes with a larger initial spot size will be a worse fit. The resist is stripped and the wafer die-sawed to produce 5 mm x 5 mm assembly templates, each containing several arrays of 1 micron deep quasi-hemispherical holes that match (to varying degrees) the 2 micron diameter polystyrene microspheres to be assembled into them.

Atomic force microscopy (AFM) is used to determine the as-fabricated profiles of the assembly sites. Figure 2 shows AFM images of four quasi-hemispherical holes, each etched from a different size starting hole in the resist. Careful attention to resist adhesion and etch procedures, along with small starting openings in the resist, enable an excellent approximation to the ideal hemispherical shape.

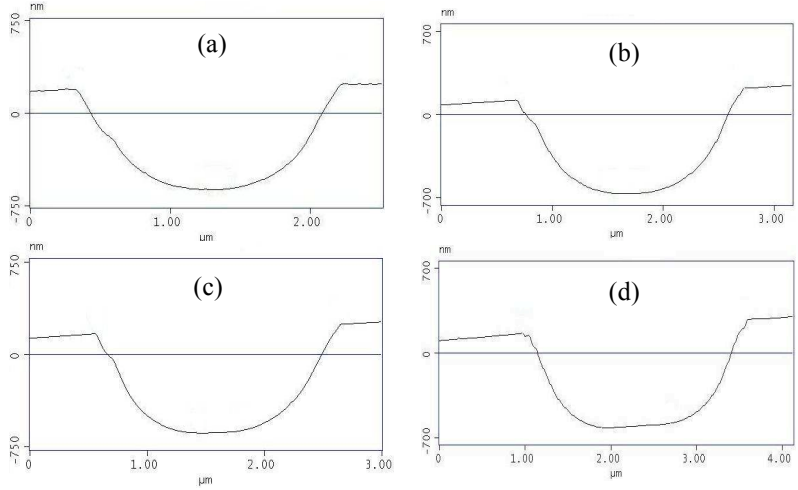

Fig. 2: AFM images of holes with starting spot sizes (from (a)-(d)) of 50, 100, 200, and 500 nm. Smaller starting hole sizes correspond to better shape matching with spherical components and therefore higher anticipated assembly yield

B) Template and component preparation

Both polystyrene microspheres and silica microspheres were assembled on TASR assembly templates in this work. The experimental protocols for the two types of spheres differ only slightly, and are based on the experimental procedure described in [1-3]. The primary difference between polystyrene assembly and silica assembly lies in the preparation of the components for assembly. An outline of the experimental protocol follows.

Since the silicon dioxide-coated template is hydrophilic, a self assembled monolayer (SAM) is grown on its surface to render it hydrophobic and to promote adhesion between the template and the hydrophobic polystyrene or SAM-coated silica components. For our experiments, SAM coating was done using octadecyltrichlorosilane (OTS); the effects of OTS on the interfacial energy with certain solvents and the coating procedure are described at length in [1-3].

Polystyrene microspheres with a diameter of 2.077 (+/- 0.045) microns were purchased dispersed in water from Polysciences, Inc. Polystyrene is naturally hydrophobic and does not need to be coated with a SAM. To prepare the assembly fluid mixture, the polystyrene microspheres were pipetted into various ethanol-water mixtures (4%, 8% and 20% water). The resulting mixture was placed in capped microcentrifuge tubes and shaken on a Vortex mixing tool (Vortex-2 Genie, by Scientific Industries) for a few minutes to disperse the components. The polystyrene component dispersions were then shaken in the ultrasonic bath for about 5 minutes to break up any agglomerates of particles. The prepared particles were used immediately to prevent re-agglomeration due to settling. For the comparison experiments with silica microspheres, the silica spheres had a mean diameter of 1.85 microns and were obtained from Bangs Laboratories Inc. (Cat. no. SSO4N). The preparation technique was essentially the same as that described in [1-3], except that the SAM-coated

microspheres were finally dispersed in ethanol-water mixtures rather than in acetone-water mixtures.

C) Self assembly protocol

A large (1325 cc) beaker was filled with water, and a 1.7 MHz frequency acoustic transducer (MMDIT-1.7, by Advanced Sonics) was placed at the bottom of the beaker. The height of water above transducer was kept fixed at about 4 cm. The input voltage (and thus power) to the transducer was controlled by a variable voltage transformer (L10C, by The Super Electronic Company). The input voltage can be varied from 0 V to 130 V, with a corresponding transducer electrical input power varying from 0 W to 36 W. The high transducer frequency ensures that operation is well below the cavitation threshold. A second, smaller beaker (the assembly beaker) was suspended above the transducer and immersed about 0.75 cm into the water in the large beaker. About 1.25 mL of the ethanol-water assembly mixture (of variable water concentration) was poured into the assembly beaker.

The template was placed in the beaker, face-up. A sufficient volume of the dispersed component mixture (between 700-800 μl) was added to the assembly beaker using a pipette. The small beaker was capped, power to the transducer was turned on, and the experiment was allowed to run undisturbed for 5 minutes. At the end of the experiment the template was taken out of the assembly mixture, placed on a flat surface and allowed to air-dry. The assembled template was then examined under an optical microscope. After the results were documented, the components were removed by 60 s of sonication in pure ethanol, and the template was reused to ensure geometrical consistency between runs. Experiments were conducted under a variety of conditions, including both polystyrene spheres and silica spheres as assembly components, different transducer voltages, different volume fraction of water in the assembly mixture, and different density of polystyrene components in the assembly mixture. The results are presented and discussed in the following section.

4. Results

The deformable polystyrene spheres were successfully and selectively assembled using TASR into matched sites in the patterned templates. After assembly, the assembly yield was quantified by calculating the ratio of the number of holes of each size that are filled with components to the total number of holes of that size. Figure 3 shows an optical micrograph of a completely filled (100% yield) array; the assembly in this case was carried out in an 8% water - 92% ethanol mixture at a transducer voltage of 45V. This template is entirely comprised of holes that were etched from 50 nm openings in the resist, so that the deviation from the ideal hemispherical shape is quite small, and the holes are extremely well-matched in shape and size to the polystyrene spheres.

Whereas the uniform array shows uniformly high assembly yield, assembly results in arrays containing holes of different sizes demonstrated selective assembly. As described previously, different sized holes were created in a single isotropic etch step by varying the size of the openings in the masking resist layer to produce features like those shown schematically in Figure 4(a). Figure 4(b) is an optical micrograph of assembly results in an array comprising four different hole sizes/shapes organized into repeating 2x2 units. The results demonstrate selective filling of four different

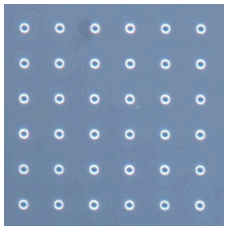

Fig. 3: Optical micrograph showing polystyrene microspheres (2 micron in diameter) self assembled on a patterned silicon template using TASR. This demonstrates 100% yield for a uniform array of holes with a starting resist opening 50 nm under these assembly conditions. Comparison with known empty holes confirms that the circular patterns in the image are filled holes rather than empty ones

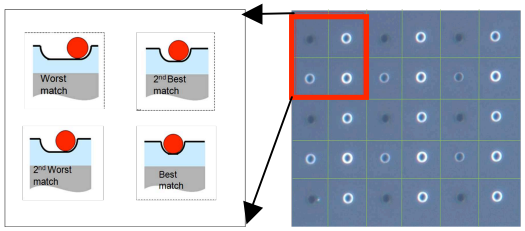

(a) (b)

Fig. 4: a) Schematic diagram of the repeated 2x2 pattern of different size/shape holes on the assembly template, with starting resist opening sizes of 500 nm (upper left), 200 nm (lower left), 100 nm (upper right), and 50 nm (lower right). b) Optical micrograph of assembly into an array of holes comprising multiple units of the 2x2 unit pattern. The holes with the largest starting size are all empty, while the better matched holes are all filled for these particular assembly parameters

hole sizes/shapes created from 50 nm, 100 nm, 200 nm, and 500 nm starting resist openings. In this particular array, the holes created from 50, 100, and 200 nm starting resist features were all filled, while the holes etched from 500 nm starting resist openings were unfilled.

To better understand the role of component deformability in the functioning of the TASR process, the variation of yield with hole size and assembly conditions was considered in the context of the original TASR model [1-3] which relates the assembly yield in part to the degree of shape matching between the undeformed components and substrate. Figure 5 shows a plot of the fractional assembly yield (where 1 corresponds to 100% yield) vs. the nominal size of the resist feature from which each hole was etched. Also plotted on the same graph is the nominal fractional contact area between an undeformed polystyrene sphere and the as-fabricated assembly site holes. To determine the nominal fractional contact area for each hole geometry, an 8th order polynomial curve fit was made to the AFM hole profiles using the surface analysis software SPIP by Image Metrology. The resulting hole shape was then compared with the sphere shape to determine the area over which the surfaces are within the contact distance (taken to be 1.5 nm), neglecting surface roughness effects. The nominal fractional contact area is then the ratio of the nominal contact area (neglecting surface roughness effects) to the surface area of the sphere.

The results confirm the expectation that a smaller starting hole size corresponds to a better component-hole match, and therefore results in higher assembly yield. The smallest resist opening size of 50 nm corresponds to a nominal fractional contact area of 0.45 and resulted in a high assembly yield of 100%. The largest resist opening size of 500 nm corresponds to a nominal fractional contact area of 0.003 and resulted in a very low assembly yield of 0.03%.

The results were then compared with the original TASR model to assess the degree to which the deformable sphere results show quantitative agreement with the

original model for rigid structures. According to the original model, the transition from zero assembly yield to 100% assembly yield is predicted by the ratio of the mechanical moments that promote component retention to the mechanical moments that promote component removal. Assembly yield increases as the moment ratio increases, with the transition from zero to full assembly centered about a moment ratio of one (the point at which retention and removal effects are equally strong).

Figure 6 plots the experimentally measured assembly yield vs. the ratio of the mechanical moments for assembly both of the deformable polystyrene spheres and of the rigid silica spheres that were assembled for comparison purposes. The silica and polystyrene assembly results exhibit similar though not identical trends of increasing yield with increasing moment ratio. It should be noted that the ratio of retention moment to removal moment has a degree of uncertainty in it due to spatial variation in the acoustic excitation in the specific apparatus used here. This would not contribute scatter to the results; rather, it would shift all of the data points to either higher or lower values of retention moment while retaining the overall shape of the assembly yield curve. Although the precise uncertainty value is not included here for the current results, it typically corresponds to about a factor of three uncertainty in either direction in the precise value of the moment ratio. Therefore, an apparent moment ratio of three in Figure 6 may in reality be as low as one or as high as eight or nine; further quantification of the uncertainty is in progress for these results. This uncertainty is consistent with the fact that the transition for silica spheres appears to be taking place at a moment ratio of about three rather than at about one as expected; within the typical uncertainty bounds, this is as expected by theory.

These results show that TASR does work with deformable polystyrene spheres despite the fact that the ratio of the interference to the critical interference for

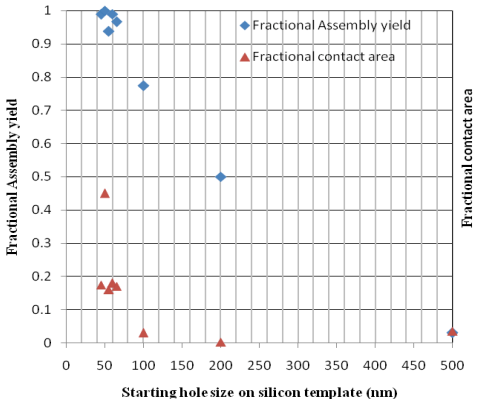

Fig.5: Plot of fractional assembly yield and fractional contact area vs the starting hole size (ranging from 50-500 nm) on patterned silicon template. As hole size increases, the contact area decreases and correspondingly, assembly yield also decreases as observed from the graph

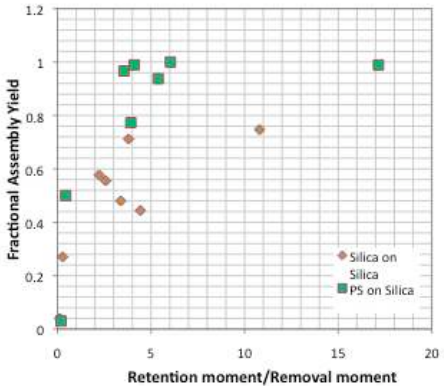

Fig. 6: Plot of fractional assembly yield vs the ratio of retention moment to removal moment with progressively decreasing hole sizes for assembly both of silica spheres on a silica-coated template and of polystyrene on a silica-coated template

polystyrene on a flat silica surface under typical TASR loads slightly exceeds the critical value of one for the onset of plastic deformation. However, the assembly results are not identical to those of silica spheres. Both the successful assembly and the deviation from silica assembly results may be addressed in the context of the Hertzian contact model presented earlier.

The degree of success in the TASR assembly is explained by the fact that the deformable spheres assembled in holes rather than on flat surfaces. The radius of curvature R_t of the assembly sites is therefore negative, leading to a much larger equivalent radius for the sphere-hole contact than for a sphere-flat contact. The larger equivalent radius of curvature decreases the ω/ω_c ratio for deformable spheres in holes as compared with deformable spheres on flat surfaces. Physically, there is less room for the extreme deformations that would lead the sphere to enter the plastic deformation regime. Table 2 summarizes the equivalent radius of curvature and the resulting ω/ω_c ratio for 2 μm diameter polystyrene spheres in holes with diameters of 2.05 μm, 2.1 μm, 2.2 μm, and 2.5 μm, which approximate the actual hole sizes on the templates. The largest value of ω/ω_c for the polystyrene spheres in the holes is about 0.15, corresponding to the largest holes. The fact that this value is significantly below the critical value of one is consistent with the experimentally observed effectiveness of TASR for the polystyrene spheres. Assembly of defect spheres on flat regions of the template may remain a concern for systems in which the interference/critical interference ratio exceeds one on the flat even when it is less than one in assembly sites. The different ω/ω_c ratios calculated for the different hole sizes also correspond to different degrees of deformation of the spheres in the different-sized holes; this is consistent with the variation in optical appearance of the polystyrene components inside holes of different sizes that is visible in Figure 4(b).

Table 2: Model results for the polystyrene-silica assembly combination, taking into consideration the hole geometry for different starting hole sizes

Starting size	R_t **(microns)**	ω/ω_c
50nm	41	0.0089
100nm	21	0.0219
200nm	11	0.0522
500nm	5	0.1502

Given that the ω/ω_c values are below one for the experimental cases considered here, one might ask why the assembly yield rises more quickly for the deformable spheres than it does for the rigid spheres in the control experiments. One possible explanation is that nanometer-scale asperities due to substrate roughness may result in a small amount of plastic deformation in the deformable spheres that enables an increase in contact surface area. At extremely short length scales, the template surface resembles a rigid surface with asperities that can indent the relatively flat surface of the deformable spheres. Even if the plastic deformation that results from nanometer-scale asperities dissipates relatively little energy overall because of the small volumes of material that are involved, it may disrupt the energy balance enough to modify the detailed assembly results as seen here.

5. Conclusions

In conclusion, we have demonstrated for the first time the successful, TASR-based, shape- and size-selective assembly of deformable microcomponents on rigid substrates. The results demonstrate both a good degree of assembly selectivity of given deformable components into different-sized holes and assembly yields of up to 100% of deformable components in well-matched holes. A theoretical model was created which complements the original TASR model and predicts the conditions under which TASR-based assembly of deformable components on a rigid substrate will be successful. The success of this model was demonstrated by comparison of the model predictions with experimental results for a component material (polystyrene) for which the material properties lie near the boundary of how much deformability can be tolerated by the TASR process. Although the assembly was essentially successful as predicted by the model, small deviations between predictions and experiments point to the need for future work to examine how plastic deformation at smaller length scales can affect the TASR process. Future work should also examine the role of deformability in the template substrate, which will be a key issue for assembly into low-cost, replicated, polymer-based templates.

Acknowledgments

All of the microfabrication was done in the Microsystems Technology Laboratories and the Scanning Electron Beam Lithography facilities at MIT. This work was supported by the National Science Foundation under Grant No 0644245, by the MIT Undergraduate Research Opportunities Program, and by a Pappalardo Graduate Fellowship.

References

[1] S. Jung and C. Livermore, Nanoletters, "Achieving selective assembly with template topography and ultrasonically induced fluid forces," Vol 5, no.11, p. 2188-94, 2005.

[2] F. Eid, S. Jung, C.Livermore, Templated assembly by selective removal: simultaneous, selective assembly and model verification, Nanotechnology 19 (2008) 285602.

[3] F. Eid, C. Livermore, Simultaneous Templated Assembly of Different-sized Nanocomponents by Selective Removal, M.S. Thesis, MIT, June 2006.

[4] Hertz, H., 1896, *Miscellaneous Papers by Heinrich Hertz*, MacMillan & Co, London, UK, p. 146–183.

[5] L.Kogut, I. Etsion, Elastic-Plastic Contact analysis of a sphere and a rigid flat, Journal of Applied Mechanics, Sep. 2002, Vol. 69.

[6] R.L. Jackson, I. Green, A finite element study of elasto-plastic hemispherical contact against a rigid flat, Journal of Tribology, April 2005, Vol. 127.

[7] Mesarovic, S. D., and Fleck, N. A., 2000, ''Frictionless Indentation of Dissimilar Elastic-Plastic Spheres,'' Int. J. Solids Struct., **37**, pp. 7071–7091.

[8] Chang, W. R., Etsion, I., and Bogy, D. B., 1987, ''An Elastic-Plastic Model for the Contact of Rough Surfaces,'' ASME J. Tribol., **109**, pp. 257 – 263

[9] Chang, W. R., Etsion, I., and Bogy, D. B., 1988, ''Static Friction Coefficient Model for Metallic Rough Surfaces,'' ASME J. Tribol., 110, pp. 57–63.